CH9900024

PSI Ber. 98-14

PAUL SCHERRER INSTITUT

PSI Bericht Nr. 98-14
Oktober 1998
ISSN 1019-0643

Nuclear Energy and Safety Research Department

On the Problem of Monitoring the Neutron Parameters of the Fast Energy Amplifier

K. Behringer and P. Wydler

Paul Scherrer Institut
CH - 5232 Villigen PSI
Telefon 056 310 21 11
Telefax 056 310 21 99

30 - 40

PSI-Bericht Nr. 98-14

On the Problem of Monitoring the Neutron Parameters of the Fast Energy Amplifier

K. Behringer* and P. Wydler

Paul Scherrer Institut

Nuclear Energy and Safety Research Department

Würenlingen and Villigen

October 1998

*Guest scientist at PSI

Preface

The proposal by a CERN group, headed by Prof. Rubbia, concerning the Fast Energy Amplifier, has received attention by politicians and government authorities. In contrast to conventional critical reactors, the Fast Energy Amplifier is subcritical and the chain reactions are maintained by supplying additional neutrons produced by a proton accelerator. The present study is concerned with the problem of monitoring the subcriticality and other neutronic parameters of this system.

Abstract

The conceptual Fast Energy Amplifier, proposed by Rubbia et al. (1995), consists of a combination of a U-233/Th-232 fuelled fast-neutron subcritical facility with a proton accelerator. An intense beam of 1 GeV protons is injected into liquid lead at the core centre and drives the reactor by producing spallation neutrons. The burst of spallation neutrons produced by a single proton alters the basic neutron statistics which are well known for thermal neutrons in conventional nuclear reactors. A short assessment of standard neutron noise analysis methods is made with respect to monitoring neutron parameter data.

Zusammenfassung

Das Konzept des Schnellen Enrgieverstärkers, welcher von Rubbia u.a. (1995) vorgeschlagen wurde, besteht aus der Verbindung eines schnellen unterkritischen, mit U-233/Th-232 beladenen Reaktors mit einem Protonenbeschleuniger. Ein intensiver Strahl von 1 GeV Protonen wird in flüssiges Blei im Kernzentrum injiziert und treibt den Reaktor durch die Produktion von Spallationsneutronen. Das von einem einzelnen Proton erzeugte Paket von Spallationsneutronen verändert die Neutronenstatistik, welche für thermische Neutronen in herkömmlichen nuklearen Reaktoren gut bekannt ist. Standardmethoden der Neutronenrauschanalyse werden für die Evaluierung und Überwachung der neutronischen Parameter kurz behandelt.

Table of Contents

List of Tables

List of Figures

I. Problem and Analytical Approach

A conceptual design of the fast energy amplifier (FEA) has been proposed by Rubbia et al. (1995) at CERN. It consists of a fast-neutron subcritical facility fuelled with U-233 and Th-232, and is cooled with liquid lead under natural convection at a temperature of about 600 °C. The driving neutron source are spallation neutrons produced by an intense beam (max. 20 mA) of 1 GeV protons from a cyclotron. The proton beam is injected in the lead coolant slightly above the core centre. The neutron lifetime (29 ns) of this system is typical for a fast reactor. For the neutron multiplication factor k, values in the range from 0.95 to 0.99 are assumed. The kinetics parameters and the subcriticality of the system are only known from core calculations, and therefore require experimental verification and subsequent monitoring. Accelerator-driven systems like the FEA may have to be equipped with a subcriticality monitoring system because the neutron source importance is sensible to beam conditions and the proton current can therefore not be used as a reliable indicator for the state of the system.

We have made a short assessment mainly of well-known neutron noise analysis methods for measuring reactor kinetics parameters. While the properties of the neutron statistics are well understood in conventional reactors, the source term of spallation neutrons alters the fast-neutron statistics. Our investigations refer to estimations in the point reactor kinetics approach using signals from a fast-neutron detector. It is obvious that any analysis time range must be short in comparison to time constants which are involved by thermal and thermal-hydraulic feedbacks.

The report is divided into the following sections:

In Section II of this report, we give relevant data for the neutron spallation process in liquid lead. Section III deals with the modified probability balance equation for the birth and death of the neutrons. From this balance equation first and second moments are obtained. Delayed neutrons are neglected, since they are of minor importance in a strongly subcritical system. Section IV is concerned with an alternative formulation of the neutron fluctuations via Langevin techniques with noise equivalent sources. For correctly establishing these noise sources we apply the results from the previous Section III. Here, we include delayed neutrons for completeness. The Langevin techniques are used for deriving various analysis methods, which are considered in Section V. Concluding remarks are given in Section VI.

II. The Spallation Neutron Process in Liquid Lead

(F. Atchison, 1998)

In order to obtain some numerical estimates for the statistics in the neutron source at the microscopic level in the FEA, a Monte-Carlo calculation with the code HETC (Chandler and Armstrong, 1972)) has been made. A large block of natural Pb with a physical density of 10.33 g/cm^3 (liquid at a temperature of 600 °C) has been assumed. 50'000 cascades, initiated by 1000 MeV protons incident normally on one open face, have been analyzed.

The average energy balance of the cascades is given in Table 1. The average distance to the first interaction is 17 cm (an interaction cross section of 1960 mb). Ionization loss makes the proton energy at the "average" interaction 748 MeV. The 5.42 interactions plus the charged particle stops (2.64 which represent medium energy particles ranged out) give an average of 8.1 secondary medium energy particles in the cascade. There are 5.6 residual nuclei from medium energy interactions (including fission products). They will be accompanied by the products arising during transport of the 29.9 fast neutrons. The "evaporation"-particle multiplicity is 31.2. Pb is weakly fissionable with medium energy protons (cross-section of order of 200 mb), and an average of 0.16 per incident proton occurs, with 2/3 of these induced by the primary proton.

Table 1: Average Energy Balance per Cascade

Events		Energy (MeV)
	Energy loss by charged particles in flight	449.2
0.16	Medium energy fission - Recoil energy	21.8
5.26	Inelastic interactions - Recoil energy	5.5
1.28	Charged clusters evaporated - Kinetic energy	67.0
29.9	Fast neutrons evaporated - Kinetic energy	99.3
	Gamma energy (neutral pions)	35.1
	Gamma energy (nuclear)	24.3
0.26	Backscattered particles - Kinetic energy	10.3
2.64	Charged-particle stops (Bragg-peak)	37.0
	Binding energy	250.5
	Total energy	1000.0

On average there are 29.9 neutrons per proton. Because of the stochastic nature of nuclear interactions, there is a large spread in the number produced; the percentage probability for producing a given number of neutrons in a cascade is shown in Figure 1. The energy spectrum of the fast neutrons is plotted in Figure 2 with 0.2 MeV wide bins. The sharp cut-off at 15 MeV is because those at higher energies have been included in the cascade calculation. The average neutron energy in the spectrum is 3.4 MeV.

The instantaneous neutron emission rates for the interaction are in the region of $10^{15}s^{-1}$ and about the same as for neutron emission in fission (the time involved in actually splitting is about 1 % of that to eject the neutrons). The time distribution of the neutrons production is mainly determined by flight distances between interactions, which are of a few cm by particles close to the velocity of light (ns region). The distribution of the time difference between the earliest interaction and latest interaction in each cascade is shown in Figure 3. Cascades with no neutron production and with 1 or 0 interaction have been eliminated. The plot is based on 45'244 cascades with time collected into 0.25 ns wide bins starting from 0.0 ns. The average time difference is 5.2 ns.

III. Modified Probability Balance Equation - First-Order and Second-Order Moment Equations

In the present approach we regard the burst of the neutrons produced by a single proton as being instantaneous, since their estimated average time-spread is fairly small compared with the neutron lifetime in the FEA. We assume that the arrival of the protons is Poissonian distributed in time. This is not exactly true, because the protons appear as periodic packages from the cyclotron (cycle frequency about 100 MHz, order of magnitude). We disregard this fine structure of the proton beam; otherwise we cannot describe the neutron process as Markovian. For simplicity, we neglect the delayed neutrons. We use the probability balance equation (for prompt effects only) given in the textbook of Williams (1974) and modify the source term. The Kolmogorov equation for the joint transition probability including a neutron detector which in the point reactor kinetics approach is considered as being uniformly distributed throughout the core, reads:

$$\begin{aligned} P(N,Z,t+\Delta t) = & \sum_{\mu=0}^{\infty} P(N-\mu,Z,t)p_s(\mu)S\Delta t + P(N+1,Z,t)(N+1)\lambda_c\Delta t \\ & + \sum_{\nu=0}^{\infty} P(N+1-\nu,Z,t)p_f(\nu)(N+1-\nu)\lambda_f\Delta t \\ & + P(N+1,Z-1,t)(N+1)\lambda_d\Delta t \\ & + P(N,Z,t)\left[1-S\Delta t-\left(\lambda_c+\lambda_f+\lambda_d\right)N\Delta t\right] \end{aligned} \tag{III.1}$$

where

$P(N,Z,t)$	=	probability that at time t there are N neutrons in the system, and that in the time interval (0,t) Z neutrons have been detected by the counting device.
S	=	average number of incident high-energy protons per unit time
$p_s(\mu)$	=	probability that μ spallation neutrons are produced in a single cascade process
λ_c	=	probability per unit time that a neutron is captured
λ_f	=	probability per unit time that a neutron induces a fission
$p_f(\nu)$	=	probability that ν prompt neutrons are produced in a single fission
λ_d	=	detection probability per unit time. It is usually expressed by $\lambda_d = \varepsilon\lambda_f$, where ε denotes the detection efficiency.

The time interval Δt is assumed to be small enough to make each of the events mutually exclusive. None of the events considered in equation (III.1) take place simultaneously in the same time interval Δt. If one takes the limit $\Delta t \rightarrow 0$, one obtains a differential-difference equation for P(N,Z,t). The treatment of this equation by the introduction of probability generating functions from which moment equations can be extracted, is described in the textbook of Williams (1974). We will give here only the final expressions. Expectation values will be denoted by an upper bar. In particular, $\overline{\mu}$ is the average number of neutrons in a spallation event, and $\overline{\nu}$ is the average number of neutrons emitted in a fission event. If one introduces the neutron absorption probability per unit time by $\lambda_a=\lambda_c+\lambda_f+\lambda_d$, and expresses the neutron multiplication factor k by $k = \overline{\nu}\lambda_f / \lambda_a$, the neutron lifetime ℓ by $\ell = 1/\lambda_a$, the neutron generation time Λ by $\Lambda = \ell/k$, and defines a positive value for the subcritical reactivity $\rho_s = (1-k)/k$, the first order moment equations read:

$$\frac{d\overline{N}(t)}{dt} = -\frac{\rho_s}{\Lambda}\overline{N}(t) + \overline{\mu}S \tag{III.2}$$

$$\frac{d\overline{Z}(t)}{dt} = \lambda_d \overline{N}(t) \tag{III.3}$$

The second-order moment equations can be written as

$$\frac{d\overline{N(t)(N(t)-1)}}{dt} = S\left[2\overline{\mu}\overline{N}(t) + \overline{\mu(\mu-1)}\right] + \lambda_f \overline{\nu(\nu-1)}\overline{N}(t) - 2\frac{\rho_s}{\Lambda}\overline{N(t)(N(t)-1)} \tag{III.4}$$

$$\frac{d\overline{Z(t)(Z(t)-1)}}{dt} = 2\lambda_d \overline{N(t)Z(t)} \tag{III.5}$$

$$\frac{d\overline{N(t)Z(t)}}{dt} = \overline{\mu}S\overline{Z}(t) + \lambda_d \overline{N(t)(N(t)-1)} - \frac{\rho_s}{\Lambda}\overline{N(t)Z(t)} \tag{III.6}$$

Equations (III.2) and (III.4), in particular, reduce under equilibrium conditions to

$$\overline{N}_0 = \frac{\overline{\mu}S\Lambda}{\rho_s} \tag{III.7}$$

$$\overline{N^2_{_0}} - \overline{N}_0^2 = \overline{N}_0\left(1 + \frac{\overline{\mu(\mu-1)}}{2\overline{\mu}} + \frac{\overline{\nu(\nu-1)}}{2\overline{\nu}\rho_s}\right) \tag{III.8}$$

where $\overline{N}_0$ and $\overline{N^2_{_0}}$ denote steady-state values.

We note, that the variance of the neutron population is increased not only by the well-known term of the fission process but also by fluctuations in the burst of spallation neutrons ever and above that for a pure Poissonian process. As expected, the spallation neutron term is not affected by the reactivity. The term vanishes, if $p_s(\mu) = \delta_{\mu 1}$ (where $\delta_{\mu\,\mu'}$ is the Kronecker symbol).

The equations (III.2 - III.6) can immediately be used in the Laplace transform to derive the variance to mean method under stationary conditions for prompt effects only.

IV. Langevin Techniques with Noise Equivalent Sources

An important method for dealing with noise problems is based on Langevin techniques with noise equivalent sources (Saito, 1974, 1979). In this approach, which is valid only for a large neutron population, the average system equations are considered as stochastic equations driven by one or more random noise sources.

We include M groups of delayed neutrons. The stochastic system equations read

$$\dot{N}(t) = -\frac{\rho_s + \beta}{\Lambda}N(t) + \sum_{m=1}^{M}\lambda_m C_m(t) + \overline{\mu}S + s(t) \tag{IV.1}$$

$$\dot{C}_m(t) = \frac{\beta_m}{\Lambda}N(t) - \lambda_m C_m(t); m = 1, M \tag{IV.2}$$

Here, we interpret N(t) as the neutron density. $C_m(t)$ is the precursor density of group m. λ_m is the decay time constant, and β_m is the fraction of delayed neutrons in group m. β is the total fraction of delayed neutrons $\left(\beta = \sum_{m=1}^{M} \beta_m\right)$. s(t) is an additive noise signal. Since we are only interested in stationary solutions, $\overline{s(t)} = 0$.

The neutron noise field of the FEA is expected to be on the microscopic level in the higher frequency region. Feedback effects, which are not included in the system equations, may appear with time constants in the order of seconds. In the high frequency region, the noise equivalent source is obtained from the Schottky formula. The auto-covariance function of s(t) is given by

$$\overline{s(t_1)s(t_2)} = \sum_i \overline{s_i^2} \delta(t_2 - t_1) \tag{IV.3}$$

where $\delta(t_2 - t_1)$ is the Dirac delta function, and

$$\overline{s_i^2} = q_i^2 \overline{x}_i \tag{IV.4}$$

q_i is the net number of events (neutrons) produced as a result of the occurrence of one nuclear reaction of type i. $\overline{x}_i$ is the average number of reactions of type i per unit time. It is assumed that each reaction type is statistically independent. We have three types of reactions:

Non fission neutron capture

$$\begin{aligned} q_1 &= -1 \\ \overline{x}_1 &= \lambda_c \overline{N}_0 \\ \overline{s_1^2} &= \lambda_c \overline{N}_0 \end{aligned} \tag{IV.5}$$

Prompt fission yielding ν neutrons

$$\begin{aligned} q_2 &= \nu - 1 \\ \overline{x}_2 &= \lambda_f \overline{N}_0 \\ \overline{s_2^2} &= \overline{(\nu-1)^2} \lambda_f \overline{N}_0 \end{aligned} \tag{IV.6}$$

Production of spallation neutrons

$$\begin{aligned} q_3 &= \mu \\ \overline{x}_3 &= S \\ \overline{s_3^2} &= \overline{\mu^2} S \end{aligned}$$

In this third case, the Schottky formula does not exactly reproduce the result from the Kolmogorov equation and the term must be replaced by

$$\overline{s_3^2} = \overline{\mu(\mu - 1)} S$$

Since the burst of the spallation neutrons occurs relatively locally, we introduce an importance factor f and write

$$\overline{s_3^2} = f\,\overline{\mu(\mu-1)}S \tag{IV.7}$$

where f is a function of the subcritical reactivity ρ_s and can be greater than 1. We obtain then for the noise equivalent source

$$\overline{s^2} = f\,\overline{\mu(\mu-1)} + \frac{\overline{N}_0}{\Lambda}\left(\rho_s + \frac{\overline{\nu(\nu-1)}}{\overline{\nu}}\right)$$

Since $\rho_s << \overline{\nu(\nu-1)}/\overline{\nu}$, and $S = \frac{\overline{N}_0}{\overline{\mu}}\frac{\rho_s+\beta}{\Lambda}$

$$\overline{s^2} \cong \frac{\overline{N}_0}{\Lambda}\left(f(\rho_s+\beta)\overline{\mu}D_s + \overline{\nu}D_f\right) \tag{IV.8}$$

where D_s and D_f are the Diven's factors defined by

$$D_s = \frac{\overline{\mu(\mu-1)}}{\overline{\mu}^2} \tag{IV.9}$$

$$D_f = \frac{\overline{\nu(\nu-1)}}{\overline{\nu}^2} \tag{IV.10}$$

A value for D_s of 1.19 has been estimated from the data plotted in Figure 1. Since the values of $\overline{\nu}$ for U-233 and U-235 are about the same, we have taken $D_f = 0.8$, which is about the accepted value in the literature.

The stationary solution of N(t) follows from

$$N(t) = \overline{N}_0 + \int_0^\infty du\, s(t-u)Q(u) \tag{IV.11}$$

Q(t) is the Green's function of the system. It represents in the frequency domain the reactivity transfer function Q(ω), where ω is the angular frequency.

$$Q(\omega) = \left[i\omega\left(1+\frac{1}{\Lambda}\sum_{m=1}^{M}\frac{\beta_m}{\lambda_m+i\omega}\right)+\frac{\rho_s}{\Lambda}\right]^{-1} \tag{IV.12}$$

Q(ω) can be represented by a partial fraction series with M+1 terms.

$$Q(\omega) = \sum_{m=1}^{M+1}\frac{q_m}{i\omega+\Omega_m} \tag{IV.13}$$

where q_m are the (real) partial fraction coefficients and Ω_m are the positively scaled (real) poles, which are all positive for a subcritical system. There are the relationships

$$\sum_{m=1}^{M+1} q_m = 1 \tag{IV.14}$$

$$\sum_{m=1}^{M+1} q_m \Omega_m = \frac{\rho_s + \beta}{\Lambda} \tag{IV.15}$$

$$\sum_{m=1}^{M+1} \frac{q_m}{\Omega_m} = \frac{\Lambda}{\rho_s} \tag{IV.16}$$

$$\frac{1}{q_j} = 1 + \frac{1}{\Lambda} \sum_{m=1}^{M} \frac{\beta_m \lambda_m}{(\lambda_m - \Omega_m)^2}; \; j = 1,\, M+1 \tag{IV.17}$$

Q(t) has then the form

$$Q(t) = \sum_{m=1}^{M+1} q_m e^{-\Omega_m t}; \; t \geq 0 \tag{IV.18}$$

If one orders the Ω_m values decreasingly, Ω_1 dominates and has the value about $\cong \frac{\rho_s + \beta}{\Lambda}$. Ω_1 is usually denoted by α. All experimental procedures which are concerned with the determination of α, belong to the class of Rossi-α methods in a broad sense.

The auto-correlation function $\overline{N(t_1)N(t_2)}$ follows from the equations (IV.3, IV.8 and IV.11)

$$\overline{N(t_1)N(t_2)} = \overline{N}_0^2 + \overline{s^2} \int_0^\infty du Q(u) Q(|t_2 - t_1| + u) \tag{IV.19}$$

To obtain the count rate (density) of the neutron detector, one has to add a virtual signal $s_d(t)$, which reproduces the detection noise term when count rates are auto-correlated. We write

$$\frac{dZ(t)}{dt} = \lambda_d N(t) + s_d(t) \tag{IV.20}$$

$$\text{where } \overline{s_d(t)} = 0 \tag{IV.21}$$

$$\overline{s_d(t_1) s_d(t_2)} = \lambda_d \overline{N}_0 \delta(t_2 - t_1) \tag{IV.22}$$

$$\overline{s_d(t_1) s(t_2)} = 0 \quad (\textit{uncorrelated}) \tag{IV.23}$$

where *s(t)* is the additive noise signal in equation (IV.1). Most of the various neutron noise analysis methods can be obtained by Langevin techniques. In a more detailed space-energy dependent treatment by using multigroup diffusion theory the Schottky formula is well applicable to absorption and fission, which are spatially uncorrelated. However, for the spallation neutron production, one has to make simplifying assumptions. The detector and its characteristics can be included as a point detector by introducing kinetic detector adjoint functions.

Table 2 gives numerical data for the six groups of the delayed neutrons for the fission of U-233 and Th-232. In our numerical estimates given in Section V we used only the data for U-233, since this dominantes the fission rate. The relatively small fission contribution of Th-232, which shows significantly higher β_m values than U-233, increases slightly the total fraction of delayed neutrons of U-233 to an effective value $\beta_{eff} = 3.30 \times 10^{-3}$.

Table 2: Delayed Neutron Data (ENDF/B-VI)

Group	U-233		Th233	
	$\beta_m(x10^{-3})$	$\lambda_m(1/s)$	$\beta_m(x10^{-3})$	$\lambda_m(1/s)$
1	0.247	53.69	0.896	53.03
2	0.658	19.95	3.096	19.79
3	0.512	5.810	4.692	5.449
4	1.009	2.422	10.836	2.109
5	0.328	0.880	4.090	0.762
6	0.117	0.284	1.987	0.246
Total fraction β	2.871		24.597	
$\bar{\nu}$ (1 MeV)	2.57		2.09	

Neutronic analyses of a 1500 MWe FEA with fresh U-233/Th-232 fuel and a neutron multiplication factor of 0.97 were performed in the framework of a doctoral thesis (Youinou, 1997). The zone-averaged neutron spectra shown in Fig. 4 were calculated by solving the inhomogeneous neutron transport equation in r-z geometry using multi-group cross-sections derived from the JEF-2.2 data library, and HETC to produce a space- and energy-dependent neutron source below 20 MeV. The geometric model is that used in the "ADS neutronic benchmark calculations" carried out in the framework of the IAEA Coordinated Research Program on the Use of Thorium-Based Fuel Cycles in Accelerator-Driven Systems to Incinerate Plutonium and to Reduce Long-Term Waste Toxicities.

It can be seen that the core spectrum of the FEA is similar to a "normal" fast reactor spectrum. The blanket and reflector spectra, however, feature a low-energy slowing-down component which becomes more significant with increasing distance from the core. Due to the low absorption and small average logarithmic energy decrement per collision in lead, neutrons in the blanket and reflector zones suffer so many elastic collisions before they are absorbed that the noise signals from detectors in these zones become insensitive to the neutronic parameters to be measured. This means that the detector has to be placed in the core.

A fast-fission detector, i.e. a fission detector using a nuclide with a fission threshold, seems to be desirable because it is insensitive to neutrons in the slowing-down region and also reduces the detector efficiency calibration problem. It should be noted that in-core fission detectors are not part of the standard fast reactor instrumentation because of the high coolant temperature of liquid-metal cooled reactors. However, high-temperature fission detectors such those developed by Trapp et al. (1996) for special flux monitoring applications should also be suitable for noise measurements.

V. Application Methods

In this section we summarize various methods for measuring the Rossi-α and the subcriticality of the FEA. The list may not be complete. In general, methods which determine directly or indirectly the Rossi-α, are insensitive for recognizing strongly subcritical states. They become sensitive when the reactor is approaching the delayed critical state. We have given a few α-values in Table 3. Conversely, methods which concern the direct or indirect determination of the subcriticality, are insensitive near delayed critical. They are sensitive in strongly subcritical states. Both classes of methods can be regarded as being complementary. For monitoring purposes, one could introduce discriminant values, a lower limit value for the Rossi-α methods, and a lower limit value for the reactivity measuring methods. Rossi-α values which scatter below the given α-discriminant value, and measured subcritical reactivity values which are below the given ρ_s-discriminant value, may indicate that the reactor is in a safe condition. For simplicity, we have not introduced importance functions and form factors, except for the spallation neutron term. This importance function is used in sensitivity studies of the Feynman method and the Bennett method. In neutron noise analysis, the detection efficiency must be high enough in order to obtain results with sufficient statistical accuracy within a reasonable measuring time. The lower limit value of ε may range in the order of 10^{-6}. The neutron detector is assumed to be of the ionization type.

Table 3: Rossi-α Values

Neutron multiplication factor k	0.95	0.97	0.99	0.999
Subcritical reactivity ρ_s/β ($)	18.33	10.77	3.518	0.349
Rossi-α (Ω_1) (rad/s)	1.818E6	1.131E6	4.428E5	1.334E5
Prompt neutron break frequency α/2 π (Hz)	2.894E5	1.799E5	7.048E4	2.123E4
Prompt neutron decay time to 10% level (s)	1.266E-6	2.037E-6	5.200E-6	1.726E-5

V.1 The Source Jerk Method for Determining the Rossi-alpha

In principle, the proton beam can periodically be interrupted for a short time. An interruption time of maximally 100 μs would be sufficient, so that the power operation is not expected to be affected. With a multichannel analyzer and a very short gate time Δt one could measure the prompt neutron decay directly.

$$\begin{aligned}\overline{\Delta Z(t)} &= \lambda_d \overline{N}_0 \Delta t;\ t<0 \\ &= \lambda_d \overline{N}_0 \Delta t e^{-\alpha t} + delayed\ neutrons + background;\ t \geq 0 \qquad \text{(V.1)}\end{aligned}$$

We must leave the technical problem of how precisely the time point t=0 can be realized, to the cyclotron specialists. The proton beam re-establishment may be another problem, since a large number of interruption cycles is required for the estimation procedure of the Rossi-α.

The gate time Δt must be less than 1 μs. A high resolution fast counting channel with a fission counter is realizable by current pulse amplification (1-2 ns rise time and bipolar delay-line clipping of a few ns). No in-core preamplifier is required which would suffer from radiation damage. The equipment developed by Behringer and Phildius (1974) allows an average counting rate of up to 10 MHz with 10% dead-time loss.

V.2 The Feynman Method (Variance to Mean Method)

The Feynman method or variance to mean method is given by

$$\frac{\overline{Z^2(t)}-\overline{Z}^2(t)}{\overline{Z}(t)}=1+\varepsilon Y_F(t) \tag{V.2}$$

where the left-hand side is a quantity to be experimentally determined, and the right-hand side is related to the Rossi-α. ε is, once again, the detection efficiency, and

$$Y_F(t)=A\sum_{m=1}^{M+1}Q(i\omega\to\Omega_m)\frac{q_m\Omega_1^2}{\Omega_m}\left(1-\frac{1-e^{-\Omega_m t}}{\Omega_m t}\right) \tag{V.3}$$

$$A=\frac{2}{\rho_s+\beta}\left(f\frac{\overline{u}}{\overline{v}}D_s+\frac{D_f}{\rho_s+\beta}\right) \tag{V.4}$$

The arrow in equation (V.3) denotes replacement. The time t has here the meaning of a gate time. If sample values $Z_n(t)$, n = 1 , ..., N_s, are measured, equation (V.2) is estimated by

$$\left[\frac{1}{N_s}\sum_{n=1}^{N_s}Z_n^2(t)-\left(\frac{1}{N_s}\sum_{n=1}^{N_s}Z_n(t)\right)^2\right]/\frac{1}{N_s}\sum_{n=1}^{N_s}Z_n(t) \tag{V.5}$$

which for a range of t values is then fitted to the theoretical expression to extract the parameter values of interest.

Equation (V.4) agrees approximately with very recent calculations given in the paper by Pázsit und Yamane (1998), who included one group of delayed neutrons in the master equation (III.1).

A VAX FORTRAN code, called FEYBEN, has been written (in double precision, 64 bits for a real number) for a numerical evaluation of Y_F as a function of the gate time t. For a run, limited numbers of different neutron multiplication factor values k and different importance function values f can be given. There are two versions with respect to the determination of the poles of the reactivity transfer function. In version 1, the denominator of Q(ω) (equation (IV.12)) has been brought into the form of a 7$^{\text{th}}$ degree polynomial. The (real and positively scaled) roots are obtained by the IMSL routine DZPORC. Version 2 determines the roots from the equation

$$1-\frac{\rho_s/\Lambda}{\Omega_j}+\sum_{m=1}^{M}\frac{\beta_m/\Lambda}{\lambda_m-\Omega_j}=0;\, j=1,M+1 \tag{V.6}$$

using repetively the IMSL routine DZBREN with given lower and upper boundary values for each root. Both versions are very fast and gave zero's which agreed within 8 digits.

The four Figures 5 - 8 show plots of $Y_F(t)$ versus gate time *t* for the cases k = 0.95, 0.97, 0.99 and 0.999. Each case includes curves with different values of the importance function *f* : 0 (lower curve), 0.5, 1.0 and 1.5 (upper curve). One can recognize that the spallation neutron variance term losses significance, as the subcriticality of the system decreases. The initial increase of the curves with increasing gate time is nearly linear. One observes then a saturation region after which a further increase due the contribution of the delayed neutrons appears. The delayed neutron effects come-up if the reactor is less subcritical. For comparison, the dashed lines show separately the prompt response. The prompt response is approximately given by

$$Y_{F(p)}(t) \cong \frac{A}{2}\left(1 - \frac{1-e^{-\alpha t}}{\alpha t}\right) \tag{V.7}$$

and may be valid up to a gate time of about 1 ms. For an estimation of α, a basic gate time of 1 μs (for k ≥ 0.97) seems to be sufficient. Today's electronics allow a simultaneous evaluation of the expression (V.5) in a large number of gate times. For the least squares fit of the data to $Y_{F(p)}(t)$ there is the boundary condition $Y_F(t=0)=0$.

An additional amplitude evaluation requires a calibration. The present concept of the FEA does not provide for control rods. In Subsection V.5 we will mention a possibility for a calibration.

The method can be made more sensitive. We propose a two-detector measuring device. The "1" in equation (V.2) is involved by auto-correlated counts and vanishes, if we combine

$$\frac{\overline{Z^{(1)}(t)Z^{(2)}(t)} - \overline{Z^{(1)}}(t)\,\overline{Z^{(2)}}(t)}{\left(\overline{Z^{(1)}}(t)\overline{Z^{(2)}}(t)\right)^{1/2}} = \sqrt{\varepsilon_1\varepsilon_2}Y_F(t) \tag{V.8}$$

where $Z^{(1)}(t)$ are the counts of detector 1 with detection efficiency ε_1, and $Z^{(2)}(t)$ are the counts of detector 2 with detection efficiency ε_2. Equation (V.8) can also be obtained from the master equation (III.1) when two detectors are included.

V.3 The Bennett Method

Rossi-α determination are also possible, if the reactor is slightly above the delayed critical state and the power increases with stable period. Under such non-stationary conditions the Feynman method diverges. Since ergodicity is violated, the theoretical expression of equation (V.2) which is based on ensemble averaging, and the experimental estimation by equation (V.5) which is based on time averaging, are not equal (Wallerbos and Hoogenboom, 1998). The divergence problem can effectively be surpressed by linear difference filter techniques (Hashimoto et al., 1998). The Bennett method is concerned with count measurements in two adjacent gate time intervals, each of length t. If $Z_1(t)$ is the number of counts in the interval (0,t), and $Z_2(t)$ is the number of counts in the interval (t,2t), the procedure is based on the estimation of $\overline{(Z_2(t)-Z_1(t))^2}/\overline{Z_1(t)}$. Bennet (1960) claims, that the difficulty of interpretation of the variance as prompt criticality is approached may be circumvented by calculating in place of variance the mean square value of the difference of integrated noise over consecutive equal time intervals. Under stationary subcritical conditions, which should be the situation with FEA, $\overline{Z_2^2}(t) = \overline{Z_1^2}(t)$. We define as the Bennet method (apart from a factor 2)

$$\frac{\overline{Z_1^2}(t) - \overline{Z_1(t)Z_2(t)}}{\overline{Z_1(t)}} = 1 + \varepsilon Y_B(t) \qquad \text{(V.9)}$$

where

$$Y_B(t) = A\sum_{m=1}^{M+1} Q(i\omega \to \Omega_m)\frac{q_m\Omega_1^2}{\Omega_m}\left[1 - \frac{1-e^{-\Omega_m t}}{\Omega_m t} - \frac{\left(1-e^{-\Omega_m t}\right)^2}{2\Omega_m t}\right] \qquad \text{(V.10)}$$

A is given by equation (V.4).

The code FEYBEN also outputs $Y_B(t)$ and the prompt response

$$Y_{B(p)}(t) \equiv \frac{A}{2}\left[1 - \frac{1-e^{-\alpha t}}{\alpha t} - \frac{\left(1-e^{-\alpha t}\right)^2}{2\alpha t}\right] \qquad \text{(V.11)}$$

The four Figures 9-12 show plots of $Y_B(t)$ and $Y_{B(p)}(t)$ for the same numerical cases as considered for the Feynman method. One can recognize that the initial (nearly linear) increase of the curves is longer and steeper than that in the corresponding Figures 5-8. The comments given in the previous Subsection V.2 also hold here. In particular, the method can be made more sensitive by using a two-detector measuring device with the combination

$$\frac{\overline{Z_1^{(1)}(t)Z_1^{(2)}(t)} - \overline{Z_1^{(1)}(t)}\,\overline{Z_2^{(2)}(t)}}{\left(\overline{Z_1^{(1)}(t)}\overline{Z_1^{(2)}(t)}\right)^{1/2}} = \sqrt{\varepsilon_1\varepsilon_2}Y_B(t) \qquad \text{(V.12)}$$

The simultaneous estimation of equation (V.9) or equation (V.12) respectively, for a range of gate times may be somewhat more complicate than in the Feynman method.

V.4 The Correlation Function Method

The correlation function method and the equivalent spectral density function method considered in the next Subsection require high detection efficiency ($\varepsilon > 10^{-4}$). The detector must be operated in the current mode (by Campelling). The momentary current at time point t is given by $I(t) = q(t)\, dZ(t)/dt$, where q(t) is the charge released per detected neutron and is an independent random variable. The auto-covariance function of the current fluctuations is defined by

$$C(t_1, t_2) = \overline{\left(I(t_1) - \bar{I}_0\right)\left(I(t_2) - \bar{I}_0\right)} \qquad \text{(V.13)}$$

where $\bar{I}_0$ is the steady state value of the current, assuming stationary conditions. C depends only on the time lag $\tau = t_2 - t_1$, and is given by

$$C(\tau) = \varepsilon\lambda_f \overline{N}_0 \left\{ \overline{q^2}\delta(\tau) + \frac{\varepsilon\overline{q}^2}{\Lambda^2} B \sum_{m=1}^{M+1} Q(i\omega \to \Omega_m) q_m e^{-\Omega_m |\tau|} \right\} \tag{V.14}$$

where

$$B = (\rho_s + \beta) f \frac{\overline{\mu}}{\overline{\nu}} D_s + D_f \tag{V.15}$$

The first term in equation (V.14) represents auto-correlated detection noise. It vanishes if one uses a two-detector measuring device. The cross-covariance function $C_{12}(\tau)$ follows from

$$C_{12}(\tau) = \lambda_f \overline{N}_0 \frac{\varepsilon_1 \varepsilon_2 \overline{q}_1 \overline{q}_2}{\Lambda^2} B \sum_{m=1}^{M+1} Q(i\omega \to \Omega_m) q_m e^{-\Omega_m |\tau|} \tag{V.16}$$

where $\overline{q}_1$ and $\overline{q}_2$ are the average charges released per detected neutron by detector 1 and 2 respectively. In the prompt neutron approximation, $C_{12}(\tau)$ reduces to

$$C_{12(p)}(\tau) \cong \lambda_f \overline{N}_0 \frac{\varepsilon_1 \varepsilon_2 \overline{q}_1 \overline{q}_2}{\Lambda} \left(\frac{\overline{\mu}}{\overline{\nu}} D_s + \frac{D_f}{\rho_s + \beta} \right) e^{-\alpha |\tau|} \tag{V.17}$$

We will comment on this method together with the following spectral density function method.

V.5 The Spectral Density Function Method

We will only consider the two-detector experiment. The cross-power spectral density (CPSD) of the current fluctuations follows from equation (V.16) by the Fourier transform.

$$S_{12}(\omega) = \lambda_f \overline{N}_0 \frac{\varepsilon_1 \varepsilon_2 \overline{q}_1 \overline{q}_2}{\Lambda^2} B |Q(\omega)|^2 \tag{V.18}$$

It reduces in the prompt neutron approximation to

$$S_{12(p)}(\omega) \cong \lambda_f \overline{N}_0 \frac{\varepsilon_1 \varepsilon_2 \overline{q}_1 \overline{q}_2}{\Lambda^2} B \frac{1}{\omega^2 + \alpha^2} \tag{V.19}$$

For the determination of the Rossi-α by least squares fit, the measurement of either $C_{12(p)}(\tau)$ (equation (V.17)) in the time domain or $S_{12(p)}(\omega)$ (equation (V.19)) in the frequency domain requires extremely high sampling frequencies of up to 10 MHz (see the data given in Table 3). This is not practicable. To our knowledge, a dual channel Fast Fourier spectrum analyzer which works in the MHz region, does not exist.

On the other hand, if one evaluates $S_{12}(\omega)$ in the plateau region of the reactivity transfer function, one has

$$|Q(\omega)|^2 \cong \frac{1}{\alpha^2}; \omega_1 < \omega < \omega_2 \tag{V.20}$$

where $\omega_1 >> \lambda_m$ + low frequencies of the power noise, $\omega_2 << \alpha$.

Since the average fission rate of $\overline{F}_0 = \lambda_f \overline{N}_0$ and the detector currents $\overline{I}_1 = \varepsilon_1 \overline{q}_1 \overline{F}_0$, $\overline{I}_2 = \varepsilon_2 \overline{q}_2 \overline{F}_0$, one obtains

$$S_{12}(\omega_1 < \omega < \omega_2) \cong \frac{\overline{I}_1 \overline{I}_2}{2\overline{F}_0} A \qquad \text{(V.21)}$$

A is given by equation (V.4). Equation (V.21) does not require a knowledge of the detection efficiencies. Since $\overline{F}_0$ represents the nuclear power and can be obtained from power balance equations, one could use the above relationship for the amplitude calibration of the Feynman or the Bennett method respectively by

$$A = \frac{2\overline{F}_0 S_{12}(\omega_1 < \omega < \omega_2)}{\overline{I}_1 \overline{I}_2} \qquad \text{(V.22)}$$

V.6 The Rossi-Alpha Method by Orndorff

This method is directly concerned with the branching process of the fission neutrons. It is especially suitable for fast reactor systems, in which the neutron lifetime is small and the nuclear chains tend not to overlap in time. The latter implies low power operation. A detector count is used to trigger a multi-channel time analyzer. If c(τ) denotes the counts following the trigger signal with the delay time τ within the time interval Δt, then we have in the prompt neutron approximation ($\alpha\,\tau \ll 1$)

$$\overline{c}(\tau) - \Delta\overline{Z} = \varepsilon \overline{F}_0 \frac{1}{2\Lambda}\left(f \frac{\overline{\mu}}{\overline{\nu}} D_s + \frac{D_f}{\rho_s + \beta} \right) e^{-\alpha\tau} \Delta t;\ \tau > 0 \qquad \text{(V.23)}$$

This equation can be derived from equation (V.17) for a detector operating in the pulse mode. It correspondingly holds for a two-detector experiment, in which the trigger signal comes from detector 1 and the following counts come from detector 2.

Figure 13 represents a block diagram of the measuring equipment used by Orndorff (1957). The trigger pulses are shaped into rectangular pulses of length Δt before they are delayed and fed to open gates of 10 coincidence counting channels. Δt was in the range of 250-500 ns. Thus, a continuous registration of delayed coincidences of counts is obtained without any loss of trigger pulses and with a dead time of only one channel width Δt. Data required from the analyzer circuit are : run time T, number of inputs N_I, number of gates N_G, and the number of counts c(τ) in each channel. The analysis gives the relationship

$$\frac{c(\tau)}{N_G} - \frac{N_I \Delta t}{T} = const(\rho_s) e^{-\alpha\tau} \qquad \text{(V.24)}$$

Normally, Orndorff used a single detector, with input 1 and input 2 tied together.

Figure 14 shows Orndorff's results from measurements made on GODIVA, a bare U-235 critical assembly, at various reactivities between delayed and prompt critical. This assembly had a neutron lifetime of 6.6 ns. The method should be applicable to the FEA (at low power) for k ≥ 0.97. The prompt neutron decay time down to a level of 10% for 4 different *k* values have been included in Table 3 (p. 14).

There are various modifications of Orndorff's measuring method, mainly with respect to the requirement in thermal reactors, where the neutron lifetime is much higher. We refer to the summary paper by Seifritz and Stegemann (1971).

V.7 The Cf-252 Method

This method is applicable to fast reactors for determining the initial subcritical reactivity (down to about k = 0.8). The proton beam remains switched-off. There is a two-detector and a three-detector measuring device. In both cases, the first detector is a fission counter coated with Cf-252, which shows spontaneous fission (half-life 85.5 y, 2.3 MeV average neutron energy). A coating quantity of 200 µg gives about 5 x 10^8 prompt neutrons. This detector is used as a random source of fission neutrons which are injected into the subcritical assembly. A spontaneous fission is simultaneously detected by one of the fission fragments (about 100 MeV in the average) emitted into the counting gas. The thickness of the coating can be made very small (about 20 µg/cm^2) so that self absorption of a fission fragment becomes negligible. Cf-252 also decays by the emission of α-particles (half-life 2.73 y, 6.1 MeV average α-particle energy). If the detector, which we call the source detector, is operated in the pulse mode, the α-particle background can be well separated by pulse height discrimination. However, for a strong source, the detector must be operated in the current mode. The second and the third detector are of the normal type of detecting neutrons. We assume that they also are operated in the current mode. Detector 2 and 3 should not be positioned too closely to the source detector, so that they do not directly register source neutrons. The Cf-252 method is superior to pulsed neutron source techniques.

V.7.1 The Two-Detector Measuring Device

The CPSD of the current fluctuation is given by

$$S_{12}(\omega) = \varepsilon_1 \varepsilon_2 \overline{q}_1 \overline{q}_2 S_{cf} \frac{\overline{V}_{cf}}{\overline{V}} \frac{Q(\omega)}{\Lambda} H_1^*(\omega) H_2(\omega) \qquad \text{(V.25)}$$

where

ε_1 = detection efficiency of the source detector for spontaneous fission of Cf-252 (≅ 1)

ε_2 = detection efficiency of detector 2

$\overline{q}_1$ = average charged released per event in the source detector (it contains α-particle background)

$\overline{q}_2$ = average charged released per detected neutron in detector 2

S_{cf} = average number of spontaneous fission per unit time in the source detector

$\overline{V}_{cf}$ = average number of prompt neutrons per Cf-252 fission (~ 3.7)

$H_1(\omega)$, $H_2(\omega)$ denote electronic flat band-pass filter function (anti-aliasing filters). We assume that these filter function are well matched, so that $H_2(\omega) = H_1(\omega) = H(\omega)$.

The method was first used for Rossi-α determinations in moderated multiplying assemblies (Mihalczo, 1970). The upper cutoff frequency of the filters must sufficiently exceed the value of the prompt neutron break frequency.

If one evaluates $S_{12}(\omega)$ in the plateau region of the reactivity transfer function $Q(\omega)$ (Seifritz, 1970) by setting

$$|H(\omega)|^2 = 1 \; ; \; \lambda_m << \omega << \alpha$$

$$= 0 \; ; \; \text{otherwise}$$

one obtains

$$S'_{12} = S_{12}(\lambda_m << \omega << \alpha) \cong \varepsilon_1\varepsilon_2\overline{q}_1\overline{q}_2 S_{cf} \frac{\overline{\nu}_{cf}}{\overline{\nu}} \frac{1}{\rho_s + \beta} \qquad \text{(V.26)}$$

The method requires a calibration for determining ρ_s. This calibration is made in conventional reactors by measuring S''_{12} at delayed critical.

$$\frac{S'_{12} - S''_{12}}{S'_{12}} = \frac{\rho_s}{\beta} \qquad \text{(V.27)}$$

One obtains directly the subcritical reactivity in $ units. However, a measurement at delayed critical is not possible at the FEA. If control rods would be present, one could try to make a calibration with a (calculated) reactivity change $\Delta\rho_s$.

V.7.2 The Three-Detector Measuring Device

The measurement of the following four spectral density functions are required:

$$S_{11}(\omega) = \varepsilon_1^2 \overline{q_1^2} S_{cf} |H_1(\omega)|^2 \qquad \text{(V.28)}$$

$$S_{12}(\omega) = \varepsilon_1\varepsilon_2\overline{q}_1\overline{q}_2 S_{cf} \frac{\overline{\nu}_{cf}}{\overline{\nu}} \frac{Q(\omega)}{\Lambda} H_1^*(\omega) H_2(\omega) \qquad \text{(V.29)}$$

$$S_{13}(\omega) = \varepsilon_1\varepsilon_3\overline{q}_1\overline{q}_3 S_{cf} \frac{\overline{\nu}_{cf}}{\overline{\nu}} \frac{Q(\omega)}{\Lambda} H_1^*(\omega) H_3(\omega) \qquad \text{(V.30)}$$

$$S_{23}(\omega) = \varepsilon_2\varepsilon_3\overline{q}_2\overline{q}_3 \overline{N}_0 \frac{D_f}{\overline{\nu}} \frac{|Q(\omega)|^2}{\Lambda^3} H_2^*(\omega) H_3(\omega) \qquad \text{(V.31)}$$

where

$$\overline{N}_0 = \frac{\overline{\nu}_{cf} S_{cf} \Lambda}{\rho_s + \beta} \qquad \text{(V.32)}$$

For the following combination of the spectral density functions one obtains

$$\frac{S_{12}^{*}(\omega)S_{13}(\omega)}{S_{11}(\omega)S_{23}(\omega)}=\frac{\overline{q}_1^2}{\overline{q_1^2}}\frac{\overline{\nu}_{cf}}{\overline{\nu}D_f}(\rho_s+\beta) \qquad \text{(V.33)}$$

This ratio of spectral density functions is independent of frequency. No correction for the frequency response of the instrumentation is required because the transfer functions for the detection system electronics are canceled. Equation (V.33) does not depend on detection efficiencies, but depends on the properties of the source detector. The ratio $\overline{q_1^2}/\overline{q}_1^2$ (Bennett factor) may be in the order of 1.2 and can be calculated. It can be optimized by constructive geometrical discrimination using the different ionization properties between a fission fragment and an α-particle.

The method does not require a calibration by the reactor. A more detailed theory which includes background fission and importance functions is given by Mihalczo et al. (1978). The determination of the extra parameters is discussed there, and results from practical applications (including statistical accuracy considerations) are presented. The greatest contribution to the statistical uncertainty comes from the estimation of $S_{23}(\omega)$. In our considerations we have neglected the variance of ν_{cf} which should give a similar but smaller contribution to $S_{23}(\omega)$ than the spallation neutron term.

VI. Concluding Remarks

The burst of spallation neutrons modifies the conventional neutron statistics and consequently influences the determination of neutronic parameters from neutron noise measurements at a FEA. The term induced by the spallation neutrons appears in amplitude relationships, but the respective measurements always require calibration because the detection efficiency is mostly unknown or not well enough determined. Rossi-α determinations are not affected by the spallation neutrons. The neutron detector must obviously be an in-core detector. An in-core fission detector which works up to 600 °C, has recently been developed at CEA (Trapp et al., 1996). This detector can be operated in the pulse mode or in the current mode. We have assumed that the detector should be a fast-neutron (threshold) detector, because the neutron energy spectrum in the FEA is hard. However, with such detectors it may not be easy to achieve a sufficiently high detection efficiency. The use of a thermal neutron detector is less attractive, because the signals may suffer from the delay-time distribution induced by the slowing-down process, meaning that Rossi-α measurements may not give representative values. Since this question cannot be answered on the basis of simple point reactor kinetics, more detailed calculations with a space-energy dependent kinetics code are desirable. Neutron noise signals measured in an accelerator-driven zero-power system or a demonstration plant (not yet existing) would also provide useful information for answering this question.

There are two classes of measuring methods. The first class is concerned with the determination of the Rossi-α. It is sensitive, if $\rho_s/\beta<1$. The Feynman and Bennett methods can also be formulated for detectors operating in the current mode. The methods of the second class are related to the determination of the subcriticality. They are sensitive, if $\rho_s/\beta>1$.

The two-detector Bennett method is believed to be most suitable for monitoring purposes. If a reliable "amplitude" calibration can be made, one could combine the determination of the Rossi-α with the determination of the subcriticality.

The present feasibility study has been undertaken to give information about the neutronic instrumentation requirements to the design engineers. Axial and radial positions should be provided for installing in-core neutron detectors in a flexible way.

Acknowledgements

The first author would like to thank Dr. P. Seiler for permission to use the PSI VAX computer system. The authors would also like to thank Dr. S. Pelloni for preparing Fig. 4.

References

Atchison, F. (1998), private communication, PSI

Behringer, K. and Phildius J. (1974), Nucl. Instr. & Methods 116, 45, EIR Report 256

Bennett, E.F. (1960), Nucl. Sci. Eng. 8, 53

Chandler, K.C. and Armstrong (1972), Oak Ridge National Laboratory Report, ORNL 4744

Hashimoto, K., Ohsaki, H., Horiguchi, T., Yamane, Y. and Shiroya, S. (1998), Ann.Nucl. Energy 25, 639

Mihalczo, J.T. (1970), Nucl. Sci. Eng. 41, 296

Mihalczo, J.T., Paré, V.K., Ragan, G.L., Mathis, M.V. and Tillett, G.C. (1978), Nucl. Sci. Eng. 66, 29

Orndorff, J.B. (1957), Nucl. Sci. Eng. 2, 450

Pázsit, I. and Yamane, Y. (1998), Ann. Nucl. Energy, 25, 667

Rubbia, C., Rubio, J.A., Buono S., Carminati, F., Fiétier, N., Galvez, J., Gelès, C., Kadi, Y. Klapisch, R., Mandrillon, P., Revol, J.P. and Roche, Ch. (1995), CERN/AT/95-44(ET).

Saito, K. (1974), Ann. Nucl. Sci. Eng. 1, 31

Saito, K. (1979), Prog. Nucl. Energy 3, 157

Seifritz, W. (1971), Reaktortagung des Deutschen Atomforums/KTG in Bonn

Seifritz, W. and Stegemann, D. (1971), Atomic Energy Review 9, 129

Trapp, J.P., Haan, S., Martin, L., Perrin, J.L. and Tixier, M. (1996), OECD Proc. Specialist Meeting on In-Core Instrumentation and Reactor Core Assessment, Mito-shi, Japan, Oct. 16-17

Wallerbos, E.J.M. and Hoogenboom, J.E. (1998), Ann. Nucl. Energy 25, 733

Williams, M.M.R. (1974), Random Processes in Nuclear Reactors, Pergamon Press, Oxford

Youinou, G. (1997), "Etudes Conceptuelle de Réacteurs Nucléaires Sous-Critiques Couplés à un Acceleratreur de Protons", Thèse soumise à la Faculté des Sciences, Département de Physique et Modélisation des Systèmes Complexes, Université de Provence.

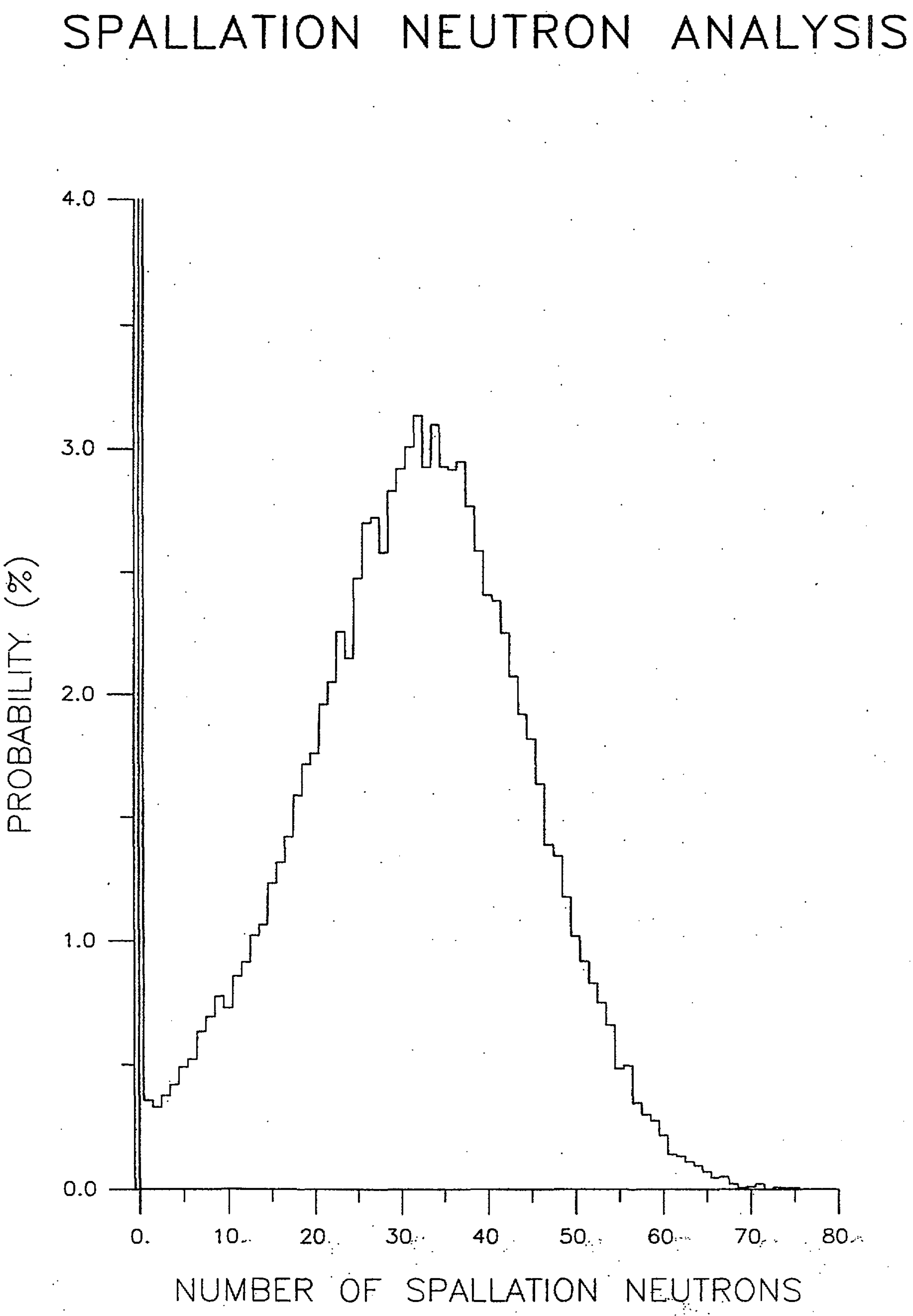

Figure 1: Spallation Neutron Distribution per Cascade

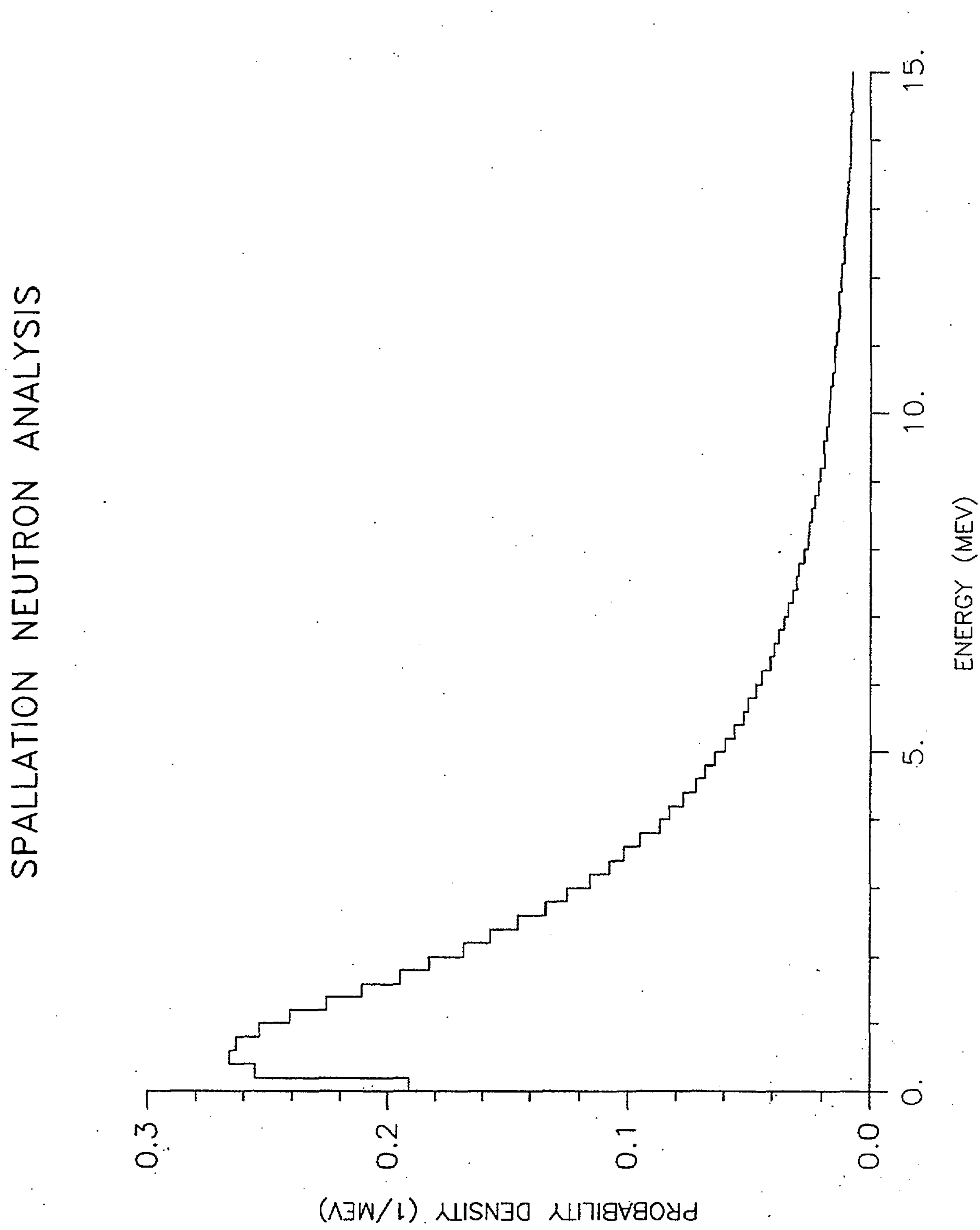

Figure 2: Energy Spectrum of the Spallation Neutrons

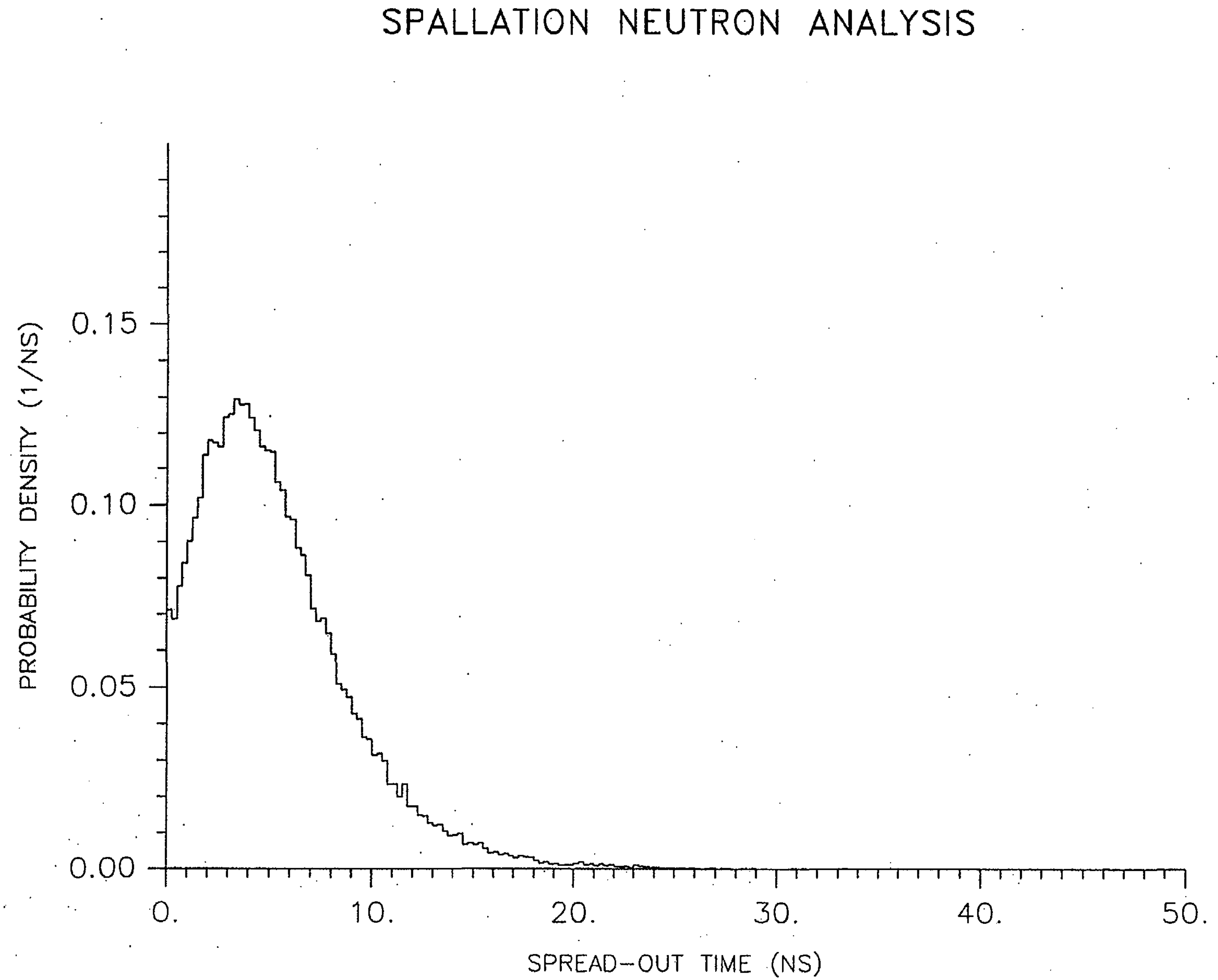

Figure 3: Spread-out Time Distribution of the Spallation Neutrons

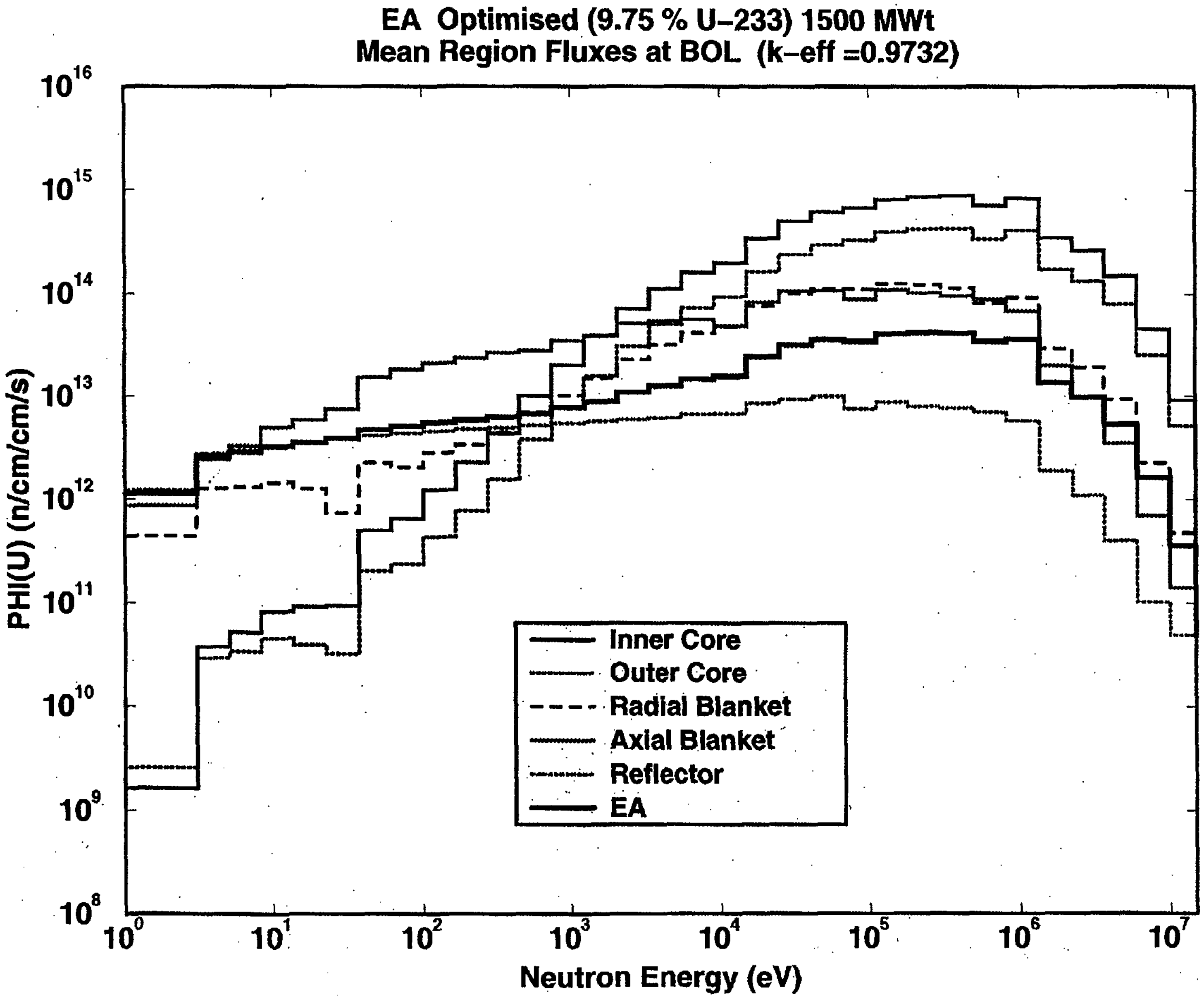

Figure 4: Mean Neutron Fluxes at the FEA in Different Zones a s a Function of the Neutron Energy

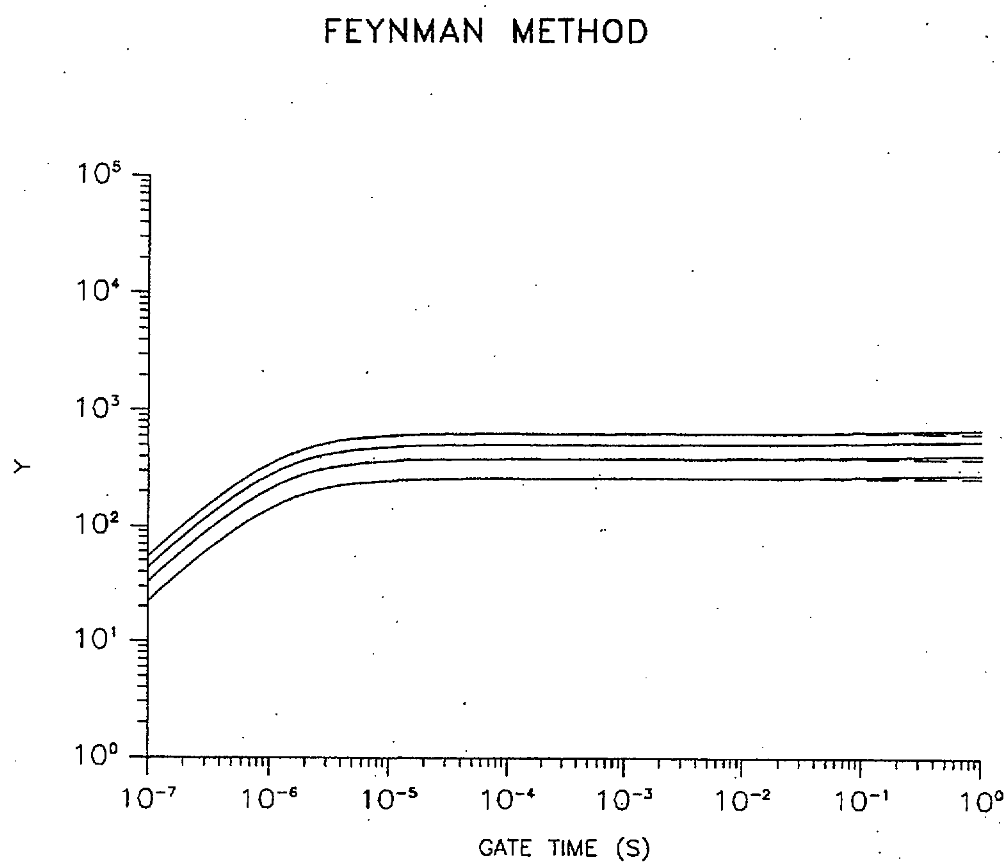

Figure 5: Feynman Y_F as a Function of the Gate Time for k = 0.95

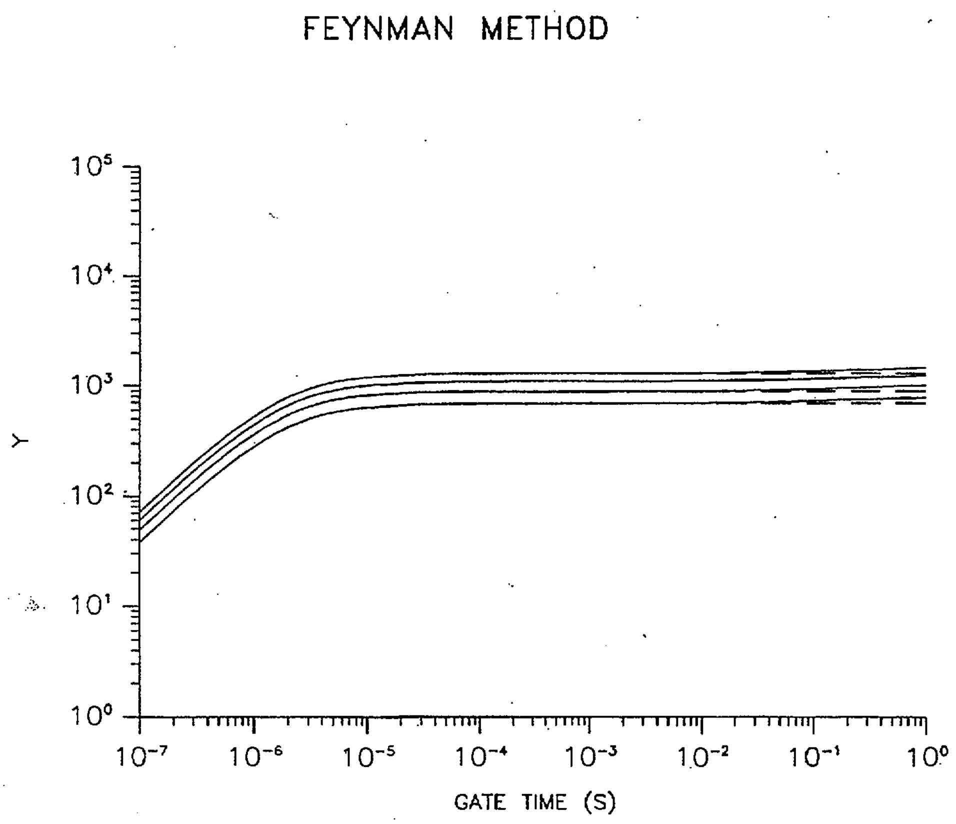

Figure 6: Feynman Y_F as a Function of the Gate Time for k = 0.97

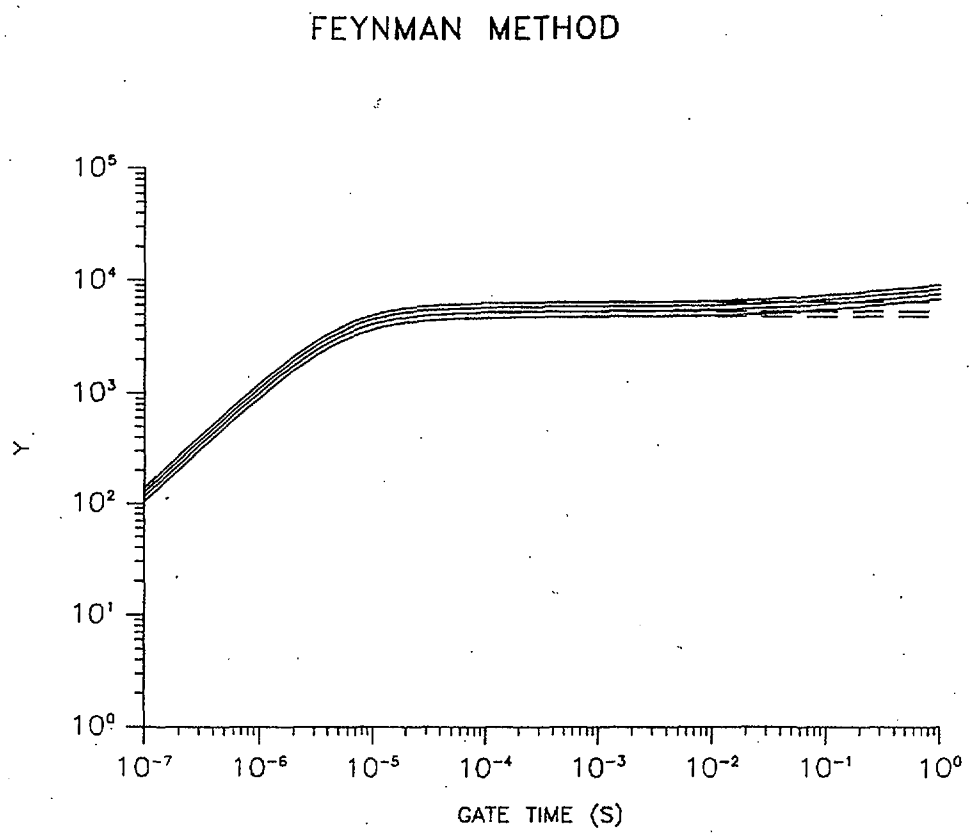

Figure 7: Feynman Y_F as a Function of the Gate Time for k = 0.99

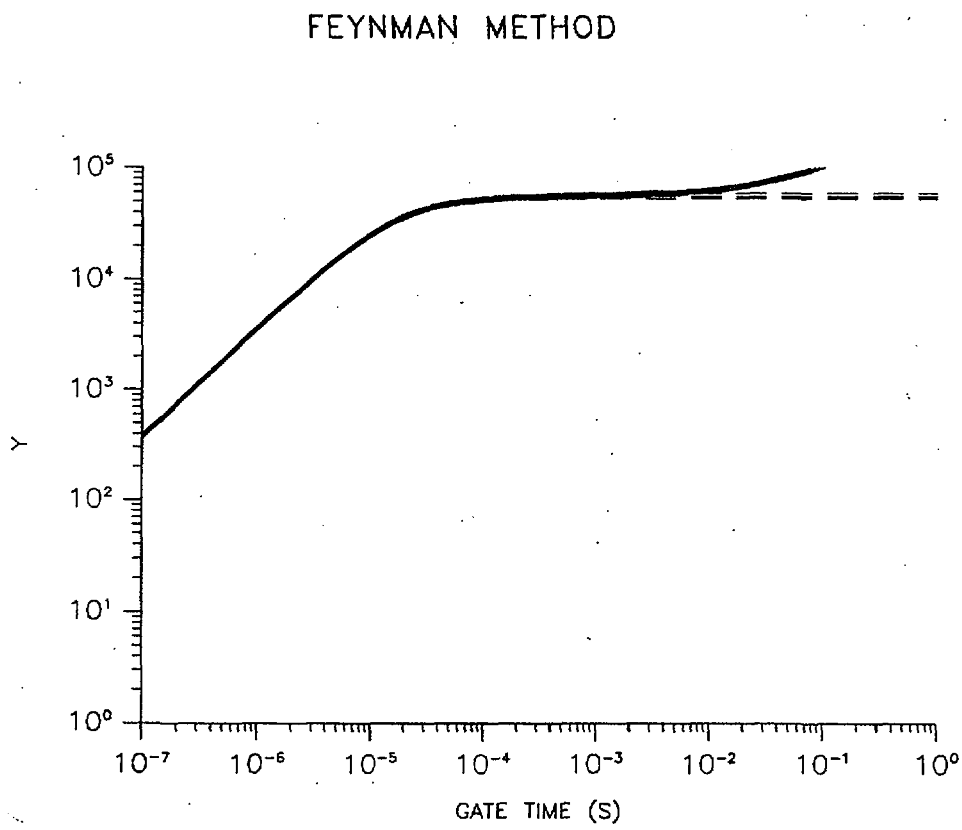

Figure 8: Feynman Y_F as a Function of the Gate Time for k = 0.999

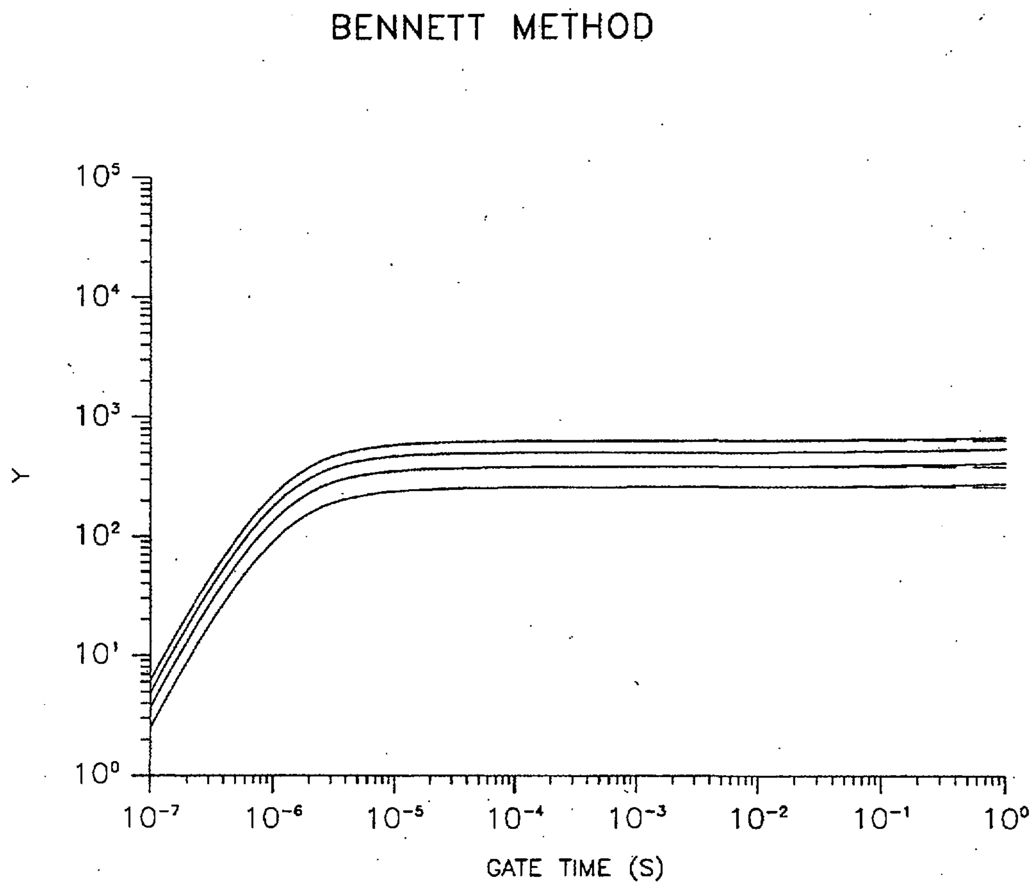

Figure 9: Bennett Y_B as a Function of the Gate Time for k = 0.95

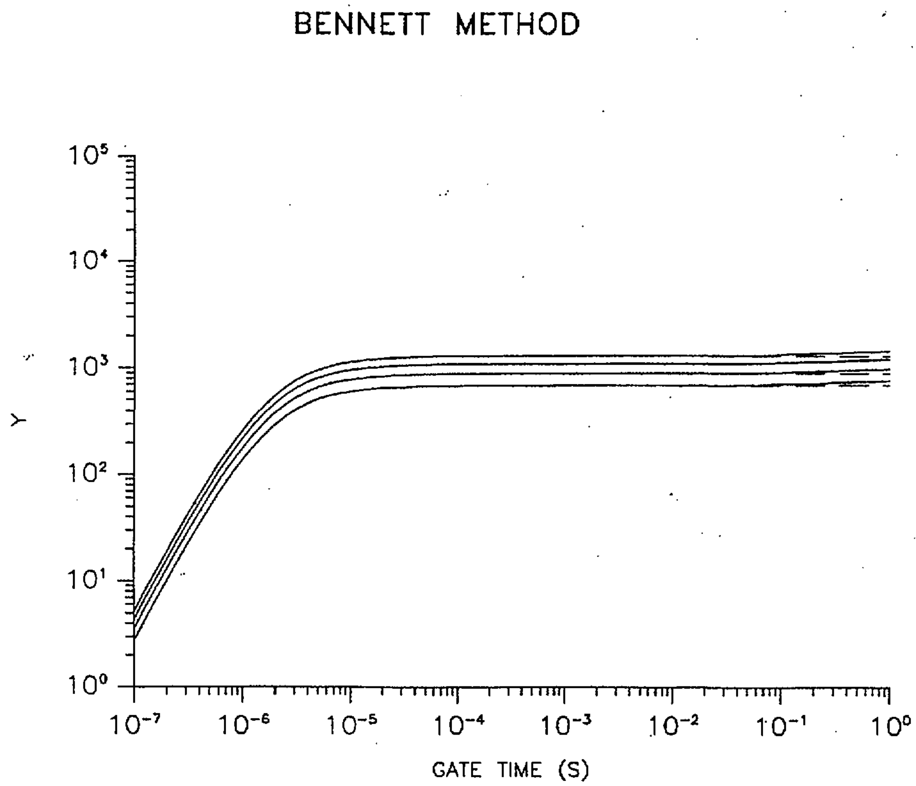

Figure 10: Bennett Y_B as a Function of the Gate Time for k = 0.97

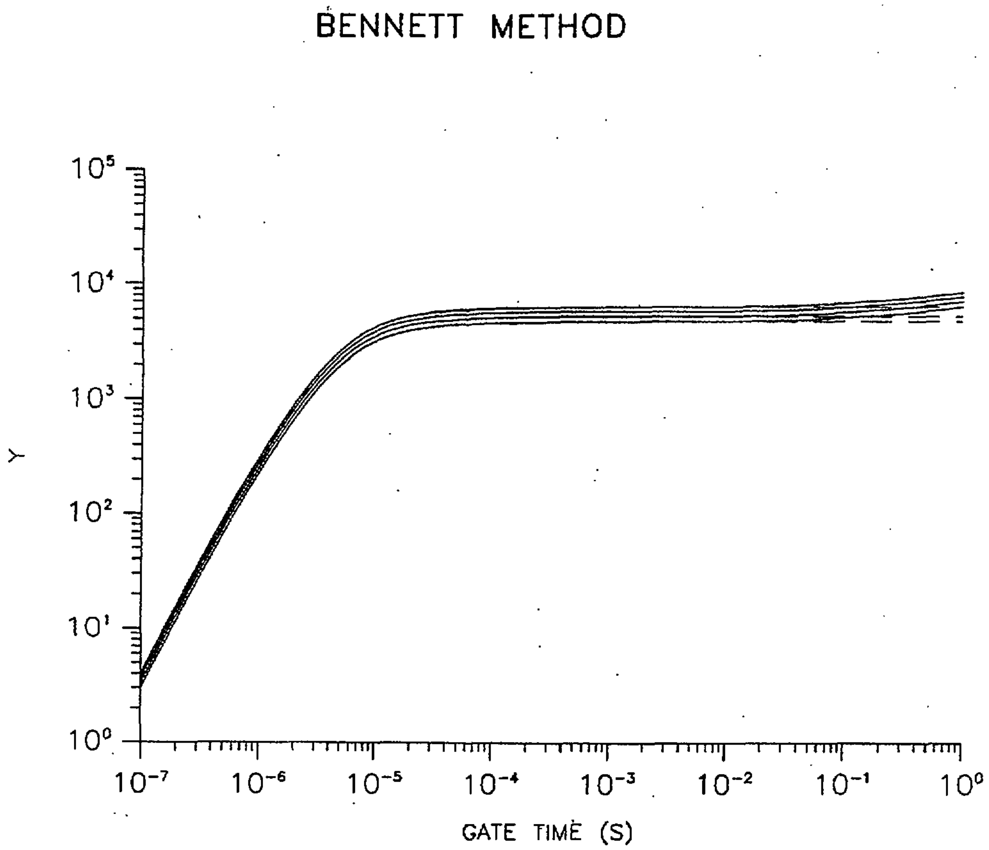

Figure 11: Bennett Y_B as a Function of the Gate Time for k = 0.99

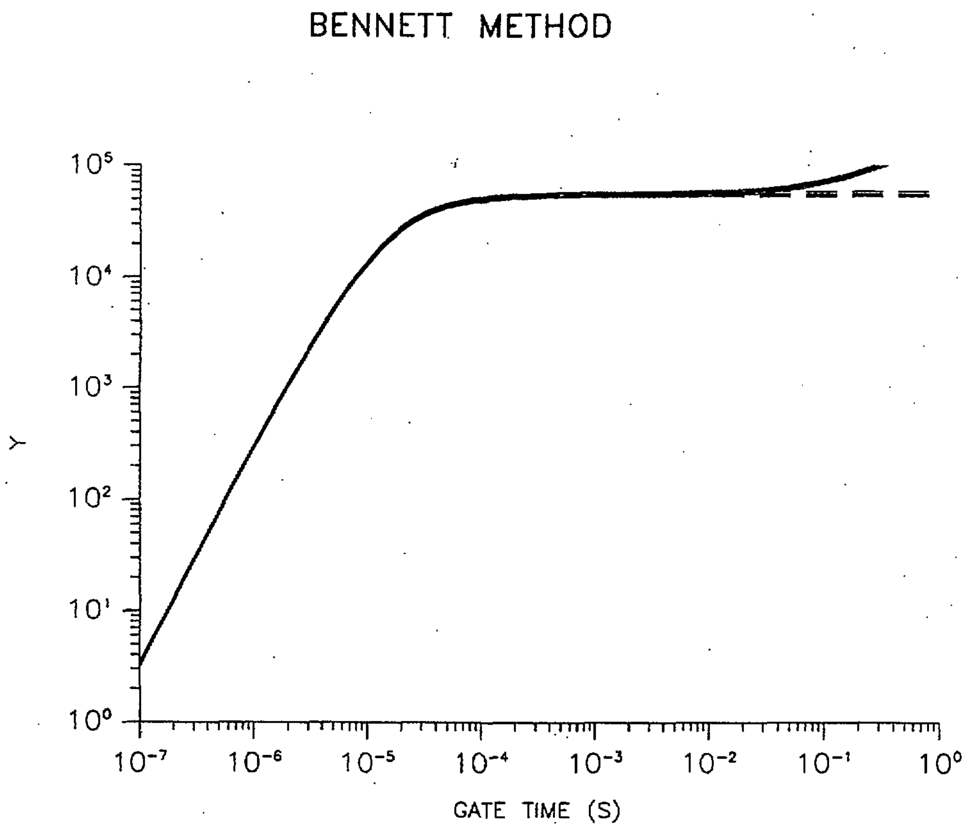

Figure 12: Bennett Y_B as a Function of the Gate Time for k = 0.999

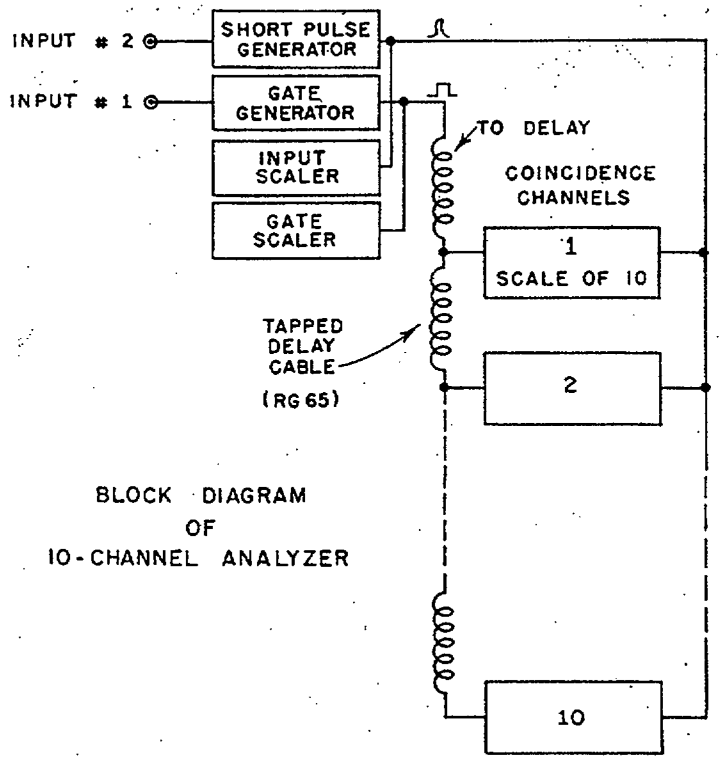

Figure 13: Block Diagram of the 10-Channel Analyzer Used by Orndorff (1957)

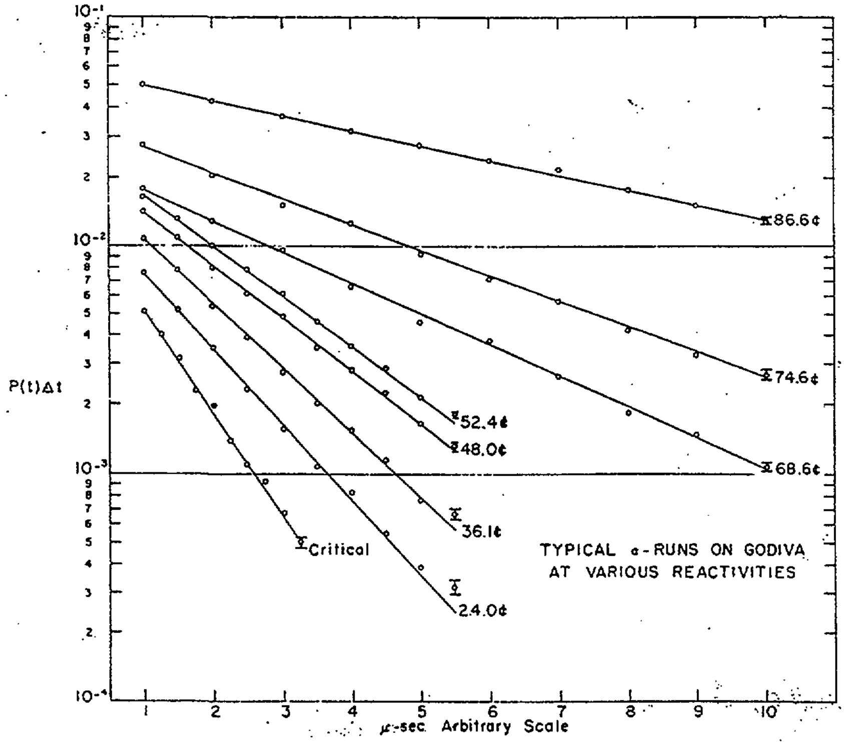

Figure 14: Typical Curves Obtained in the Rossi-Alpha Experiments on GODIVA at Various Reactivities (from Orndorff, 1957)